

Improvements of torque ripple reduction in DTC IM drive with arbitrary number of voltage intensities and automatic algorithm modification

Marko ROSIĆ^{1,*}, Sanja ANTIĆ¹, Milan BEBIĆ²

¹Department of Power Engineering, Faculty of Technical Sciences Čačak, Univeristy of Kragujevac, Čačak, Serbia

²Department of Power Converters and Drives, School of Electrical Engineering, University of Belgrade, Belgrade, Serbia

Received: 02.03.2020

Accepted/Published Online: 29.07.2020

Final Version: 30.03.2021

Abstract: Techniques of direct torque control (DTC) are very common in high-performance electric motor drives. Retaining the good features of the conventional DTC and reducing torque ripple have been the subject of many years of research work on improving these algorithms. This paper presents the DTC algorithm with discretized voltage vectors based on the use of conventional switching table (ST-DTC). This algorithm enables a significant torque ripple reduction by defining the corresponding number of the given voltage intensity while retaining calculation simplicity and fast torque response typical of the ST-DTC algorithms. The proposed algorithm has the ability for its automatic modification depending on the defined number of voltage intensities by the user. In a simple way, the proposed algorithm enables the influence compensation of the induced electromotive force for a torque error at high speed. Experimental results obtained by using MSK2812 digital control platform confirm the significant reduction of the torque ripple with an increase of the number of defined voltage intensities.

Key words: AC motor drive, variable speed drive, direct torque control, torque ripple reduction, electromotive force compensation

1. Introduction

Unlike a large number of direct torque control (DTC) algorithms with a continuous voltage vector [1–3], the switching table DTC algorithm (ST-DTC) is set apart through simplicity, less sensitivity to machine parameter variations, and exceptionally good dynamic properties. The negative side of these algorithms is a relatively large torque ripple as a result of nonlinear control and applying a small number of discretized voltage vectors of maximum intensity. For this reason, a lot of scientific effort has been invested in solving this problem [4]. In [5–8], several modifications of the switching tables and the flux and torque regulators have been put forward, which should provide the ripple reduction and thus eliminate the torque error in the steady state. The key for performance enhancement of ST-DTC algorithms, i.e. significant reduction of the flux and torque ripple lies in increasing the number of available active voltage vectors (intensities). In [9], the authors proposed the application of two voltage vectors in the ratio of 50%–50% within the time-span of one voltage vector. Torque ripple has been reduced almost two times by applying this method, better known in the literature as the discrete space vector modulation direct torque control (DSVM-DTC). Further in the solutions proposed in [10–12], the DSVM-DTC calculation cycle is divided into three segments within which three corresponding voltage vectors are applied. In this way, the number of available active voltage vectors is increased from the perspective of the

*Correspondence: marko.rosic@ftn.kg.ac.rs

entire calculation cycle. Although the torque ripple has been significantly reduced with further increase in the number of voltage vectors, in this way, the switching tables can become complicated and the calculation cycle duration needs to be extended in order to prevent excessive switching frequency (shifting four or more voltage vectors in one calculation cycle).

It can be said that the development of converters with more voltage level has enabled further survival and development of ST-DTC algorithms particularly when it comes to multilevel inverters and multiphase machines [13]. With an increase in the number of levels in the multilevel inverter [14, 15], the resulting voltage vector approaches the continuous voltage vector, which favorably affects the torque ripple intensity. Still, in addition to simplicity of these methods and advantages in terms of a smaller voltage slew-rate (du/dt), a too great number of the available voltage intensities can lead to challenges in selecting the voltage vector if good dynamic properties of the drive ought to be maintained. Having higher density voltage vector production with multilevel inverters, usually next applied voltage vector is closest appropriate vector that belongs to one corner of elemental hexagon surrounding the reference voltage vector at the moment. This reduces high dynamics in torque response and overall system bandwidth due to possible large changes in torque reference [16]. Switching tables for inverters with more than 3 voltage levels have become very complex due to which their utilization in practical implementation is rare. For this reason, with a greater number of inverter voltage levels, different principles are approached for selecting voltage vectors that render the original simple principle more complex or reduce the bandwidth of the system by selecting an adjacent voltage vector [17]. Multiphase machines and corresponding inverters also provide a better spatial resolution of the voltage vector leading to the torque ripple reduction [18–20]. However, multiphase machines are still not in the wider commercial production and use, which reduces the attractiveness of such solutions.

A very important aspect of DTC algorithms is their complexity. Preserving calculation simplicity of DTC algorithms and reducing dependence on machine parameters contributes to the popularity of its implementation in industrial controllers today. Also, preserving calculation simplicity and enabling greater resolution in control [21] reduces the regulation error due to digital implementation [22]. Flux estimation is in the basis of all DTC algorithms. Maintaining the simplicity of the DTC algorithm itself leaves a computational space for the implementation of more complex calculations requiring advanced flux estimators, or drive parameter state observers [23]. A general conclusion can be drawn that the simplicity of DTC algorithms is a desirable feature. This paper presents an algorithm based on the principles of a conventional DTC with switching table that feature extremely low calculation times. The proposed algorithm allows the definition of multiple discretized voltage intensities (DVI-DTC) with a standard two-level voltage source inverter. The DVI-DTC algorithm retains the use of a conventional switching table that defines the direction of one of the six basic voltage vectors (with a choice of several different intensities) thereby preserving the simplicity of selecting a voltage vector. In [24], DTC with virtual voltage vectors is presented in order to increase a number of voltage vector directions and further reduce the torque ripple. On the other hand, the authors in [25] provide results confirming that the degree of the torque ripple reduction in the ST-DTC algorithms does not depend on the choice of voltage vectors of different directions to such extent as the choice of vectors of different intensities. For this reason, retaining a conventional switching table with six basic directions of voltage vectors can be considered as justified. The effect of an induced electromotive force (EMF) on the stationary torque error is expressed for all ST-DTC algorithms, particularly at high speeds. The proposed DVI-DTC facilitates simple compensation of the influence of EMF and elimination of torque errors in steady state while retaining calculation simplicity and high torque dynamics. Also, the DVI-DTC algorithm has the possibility of automatic modification according to the defined

requirements in terms of the maximum allowed torque ripple of a machine. With the aim of reducing the torque ripple, the user can select an appropriate number of voltage intensities and the algorithm will automatically redefine the corresponding intensities of voltage vectors as well as the levels and limits of the torque comparator. This is possible due to the fact that the switching table does not change depending on the number of available voltage intensities opposite to [24] where further increase of virtual voltage vectors requires definition of new and more complex switching tables.

The paper is structured as follows. Section 2 describes the principles of DTC with discretized voltage intensities and its automatic modification procedure depending on the defined number of voltage intensities. Speed impact on torque increments during a switching cycle is analyzed in Section 3. In Section 4, experimental results are provided to substantiate the effectiveness of the proposed DVI-DTC algorithm with compensated EMF impact. Degree of torque ripple reduction depending on available voltage intensities is analyzed with and without EMF compensation. Finally, Section 5 summarizes the conclusions.

2. Principles of direct torque control with discretized voltage intensities

The conventional DTC principles are widely known and elaborated in a large number of publications [26]. The structure of a standard voltage inverter provides six active voltage vectors spatially displaced to $\pi/3$ sufficient to form a rotational magnetic field. Voltage vector direction is determined by demands for torque (D_T) and flux (D_Ψ) as well as the sector (S) where the stator flux $\Psi_s(t)$ is located. The consequence of such extremely nonlinear control and application of only six active voltage intensities lead to a very distinct torque ripple and flux as well as a variable switching frequency.

2.1. Application of discretized voltage vector intensities DTC

In order to reduce torque ripple by increasing the number of available voltage intensities in this paper, an algorithm with discretized voltage vector intensities (DVI) is proposed. The DVI-DTC algorithm is based on defining more diversified intensities of the six basic active inverter vectors obtained by fixed frequency pulse width (PWM) modulation as shown in Figure 1.

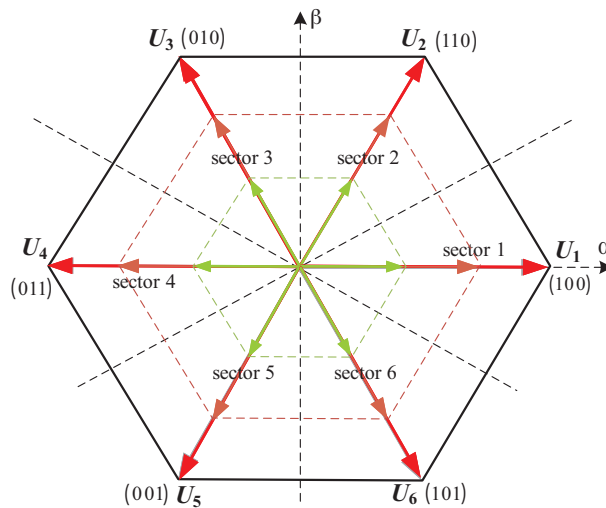


Figure 1. Multiple (three) discretized voltage vector intensities.

By determining the duty ratio of each voltage vector, it is possible to predefine an arbitrary number of intensities without the use of multilevel inverters or a combination of several basic voltage vectors as in the DSVM-DTC. The available voltage intensities are predefined (before the DTC algorithm starts), where each component of available voltage vector is already calculated and set to be used by PWM unit. In this way, the number of possible voltage vectors is theoretically limited by the characteristics of the processor's counting module and its clock frequency. Moreover, the problems related to variable switching frequency of conventional DTC which depend on motor speed and hysteresis comparators bandwidth are removed. Defining a higher number of available voltage intensities in this way allows us to keep the conventional DTC switching table and the simplicity of the voltage vector selection. Increase in number of available intensities improves only voltage vector resolution in each of six basic directions, without affecting the PWM switching frequency, which will finally result in reduced torque ripple. By applying a different intensity of a voltage vector, it is possible to provide a different angle between stator and rotor flux vectors within the time Δt . In this way, depending on the intensity of the torque error, it is possible to choose the appropriate voltage vector to be applied at the next sample. For this reason, the conventional three-level torque comparator must be modified and expanded. In order to recognize the torque error depending on the number of predefined voltage intensities, it is necessary to define a torque comparator with an appropriate number of levels.

2.2. Multilevel torque comparator and automatic algorithm modification procedure

If, for example, three active voltage vectors of the same direction are available, it is necessary to define a 7-level torque comparator. This comparator can be of a hysteresis or nonhysteresis type as it is presented in Figure 2.

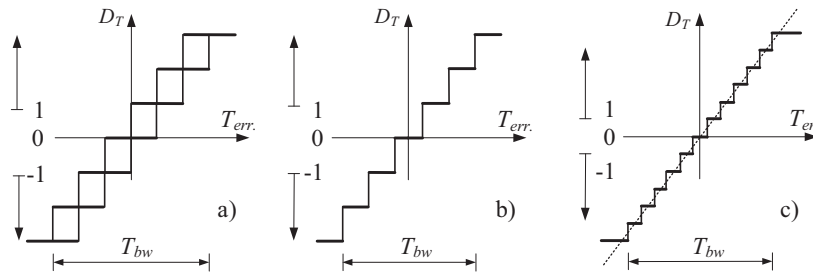


Figure 2. Hysteresis (a) and hysteresisless torque comparators with 7 (b) and 13 (c) levels.

Having in mind the available number of defined voltage vector intensities, the hysteresis type of the torque comparator raises some questions. Namely, with the introduction of a PWM, the switching frequency becomes constant; the hysteresis effect at the boundary of the comparator level loses its significance. The intensity of the selected voltage vector should correspond to the range in which torque error is present, so the intensity of the vector can be changed faster (between adjacent values) without the hysteresis effect of the comparator. This is especially important with large number of available voltage vector intensities, that is, with higher number of comparator levels. By increasing the number of torque comparator levels and the available voltage vectors in this way, the functioning of the described torque regulator approaches the principle of operation of the linear proportional torque regulator, with continuous voltage output (Figure 2c). Also, by increasing the number of voltage vectors, the difference between adjacent intensities is reduced, resulting in lower torque ripple. In this way, it is possible to define a favorable number of available voltage vector intensities that will fulfill the requirements for the permitted (desired) torque ripple in the drive. With conventional DTC, the torque control was carried out by a hysteresis comparator with three levels of width T_{bw_c} . The width of the corresponding

torque comparator for the proposed DVI-DTC structure with multiple levels T_{bw_p} is determined as follows:

$$T_{bw_p} = \frac{T_{bw_c}}{3} \cdot n = \frac{T_{bw_c}}{3} \cdot (2 \cdot i + 1), \quad (1)$$

where n is the number of levels in torque comparator, and i is the number of voltage vector intensities in the DVI-DTC structure. A multilevel torque comparator defined in this way is presented in Figure 3.

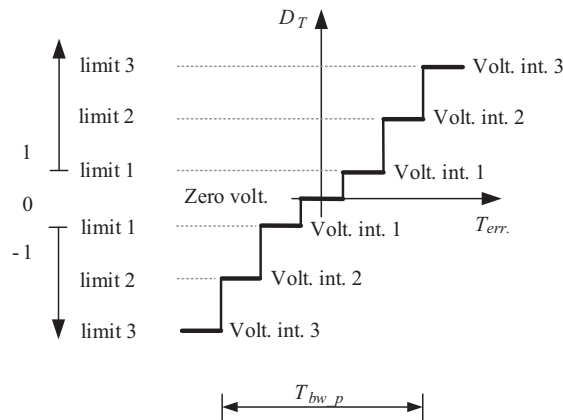


Figure 3. 7-level hysteresisless torque comparator.

The important characteristic of the proposed control structure is the separate (decoupled) selection of the direction and of the intensity of the voltage vector. This feature makes it possible to hold the conventional switching table in charge of selecting the direction, while the multilevel torque comparator is responsible for selecting the intensity of the voltage vector. In this way, in order to further reduce the torque ripple, it is possible to simply extend the control structure to a greater number of available voltage intensities, which only modifies the torque comparator and not the switching table. Moreover, this modification of the algorithm with increasing number of voltage vector intensities can be automatized depending on the highest acceptable torque ripple. This automation should provide the solution for two tasks: i) defining the required discretized voltage intensities; ii) the appropriate modification of the torque comparator. If, for example, the proposed DTC algorithm should have $i=5$ voltage vector intensities, the automation of these two tasks is reduced to:

i) Predefine the discretized voltage vectors intensities. This can be accomplished by dividing the maximum intensity (corresponding to PWM duty ratio) into 5 equal parts. In this way, the available intensities would be: 0%, 20%, 40%, 60%, 80%, and 100% of the maximum available voltage;

ii) Predefine the appropriate torque comparator - similar to division of intensities, the torque comparator values should also be equidistant. The width of the torque comparator (1) should be divided into $2 \times i - 1 = 9$ parts, which would define the boundaries of individual levels (T_{bw_i}) of the $n = 2 \times i + 1 = 11$ - level torque comparator. Each of these levels would correspond to one of the 5 defined voltage vector intensities and one zero voltage vector.

Having in mind above stated, automatic algorithm modification procedure of DVI-DTC is shown in Figure 4a.

In this way, the modification of the algorithm, depending on the number of required voltage intensities, is straightforward and fast. Modifications related to selection of different switching tables (predefined look-

up table), adapted to the number of levels in the comparator, have been avoided. Also, with the increase in the number of discretized voltage intensities and consequently number of levels in the torque comparator, the nonlinear nature of torque control (with conventional DTC) is increasingly approaching the linear controller (for $n \rightarrow \infty$). This feature of the proposed algorithm shows its good properties in cases when a user wants to adapt the drive to the requirements with regard to the reduction of the torque ripple. If the DTC drive operation results in a large torque ripple, it is possible to bring the torque ripple to a satisfactory level simply by increasing the number of desired voltage intensities (Figure 4a). Simplicity of the conventional DTC algorithm with low calculation time is retained, while the ability to arbitrarily reduce torque ripple depending on the number of applied discretized voltage intensities is gained. Based on the above, the proposed algorithm with DVI-DTC with a multilevel torque comparator can be represented by the block diagram shown in Figure 4b.

The last block, before the PWM unit, in Figure 4b represents the block which enables EMF compensation and will be described in the next section. Simulation results of stator flux locus in α/β reference plane with conventional DTC and proposed DVI-DTC are shown in Figure 5. The results confirm significant reduction of stator flux ripple with DVI-DTC with 4 voltage vectors.

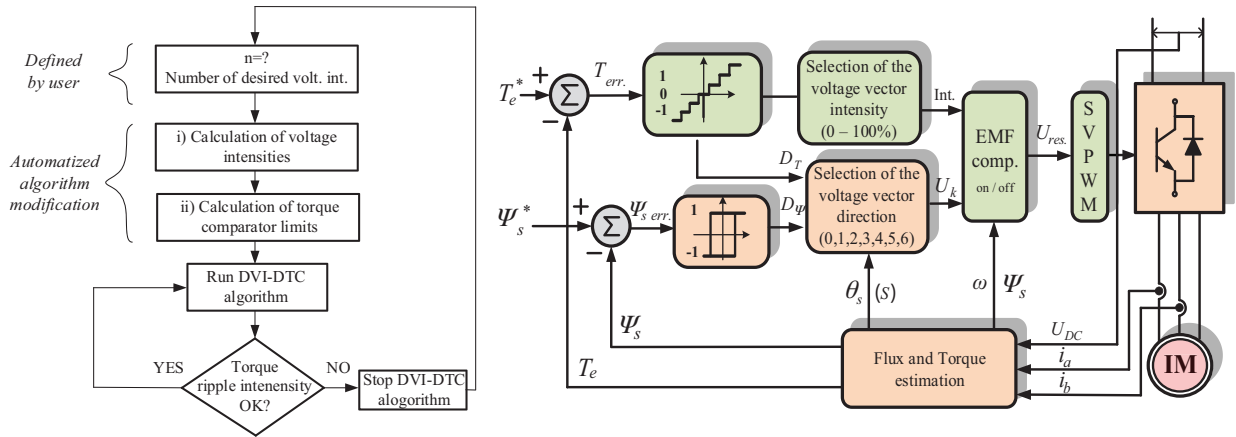


Figure 4. The flowchart of automatic algorithm modification (a) and block diagram of DVI-DTC algorithm (b).

3. Compensation of speed impact on torque response

3.1. Speed impact on torque increment analysis

The torque increment intensity ΔT_e within a sampling time Δt is significantly influenced by the motor speed. The induced electromotive force reduces positive torque increments as motor speed rises (Figure 6), which leads to the occurrence of a torque steady-state error that becomes noticeable at high speeds. Starting from the general mathematical model of the machine in the $\alpha\beta$ plane, it is possible to reach the relations that define the increment of the torque during time Δt [12, 27]. The resulting torque at the next sample $T_e(t + \Delta t)$ consists of three members according to the expression (2):

$$\Delta T_e(t + \Delta t) = T_e(t) + \Delta T_{e1}(t) + \Delta T_{e2}(t); \tag{2}$$

$$\Delta T_{e1}(t) = -T_e(t) \left(\frac{1}{\tau_s} + \frac{1}{\tau_r} \right) \frac{\Delta t}{\sigma}; \quad \sigma = 1 - \frac{L_m^2}{L_s L_r}; \tag{3}$$

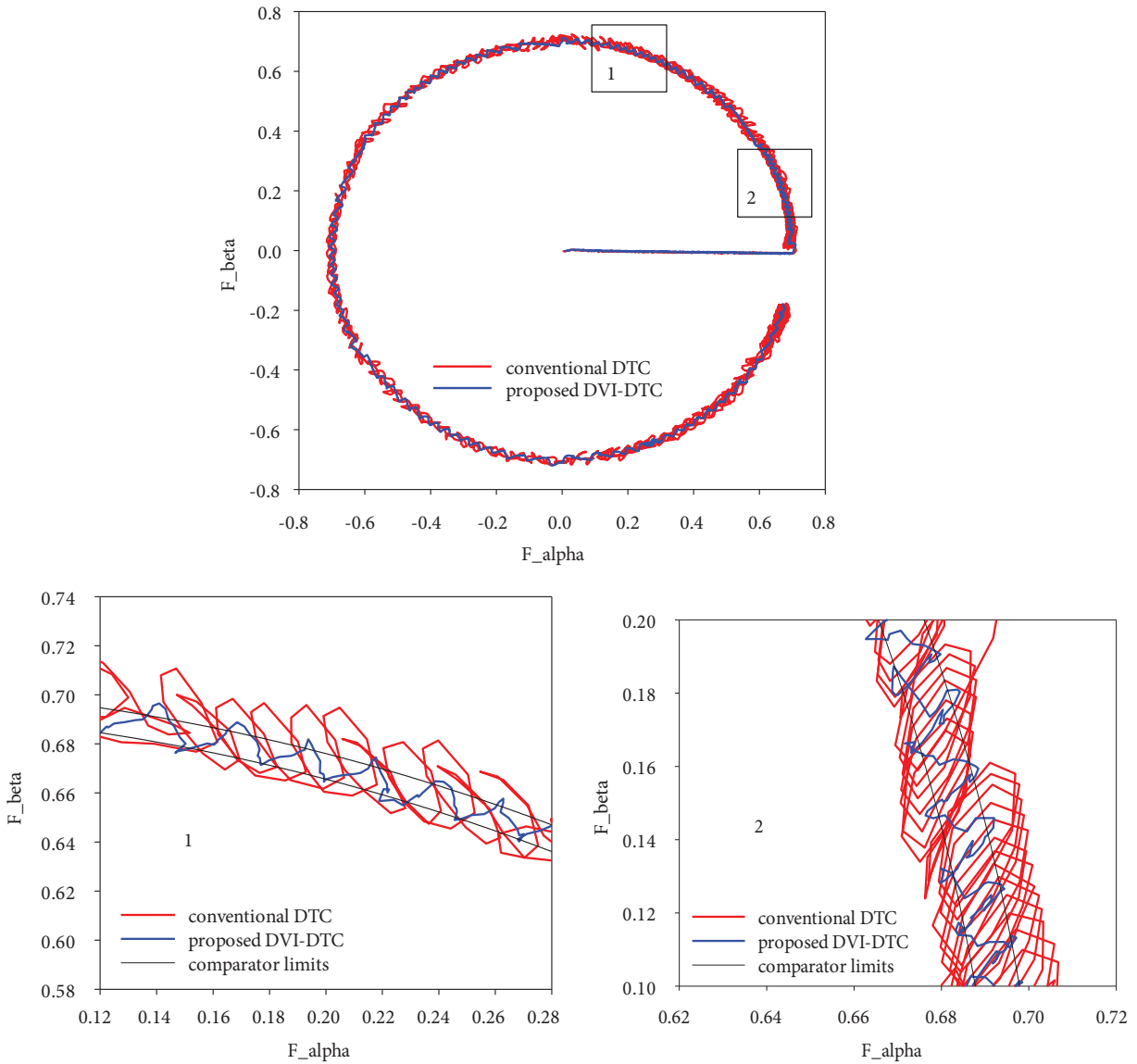


Figure 5. Locus of the stator flux with conventional and DVI-DTC.

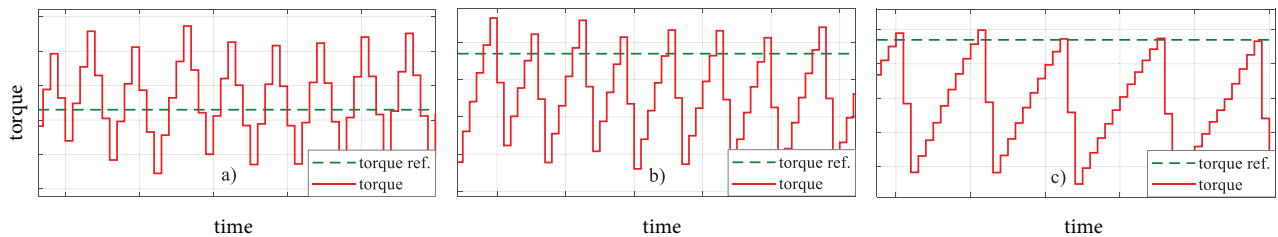


Figure 6. Waveforms of estimated torque sampled at Δt for (a) low speed, (b) medium speed, and (c) high speed.

$$\Delta T_{e2}(t) = \frac{3}{2} p \frac{L_m}{\sigma L_s L_r} [(\mathbf{u}_s(t) - j\omega(t) \Psi_s(t)) \cdot j\Psi_r(t)] \Delta t, \quad (4)$$

where p is number of pole pairs; L_m, L_s, L_r are mutual, stator, and rotor inductance; ω is motor speed; Ψ_s, Ψ_r are stator and rotor flux vector; τ_s, τ_r are stator and rotor time constants, and \mathbf{u}_s is stator voltage vector.

The first term in expression (2) is the value of the machine torque at the beginning of the cycle at time t , the second term (3) represents a torque weakening which depends on the machine parameters. The third term (4) is torque increment due to applied stator voltage and induced EMF during Δt . In order to make the effect of the resulting voltage clearer, the torque increments ΔT_{e2} were calculated using (4) for different directions (angles) of the full stator voltage vector, with respect to the angle of the rotor flux.

Figure 7a displays the graphic representations of torque increments ΔT_{e2} for the induction machine the data of which have been given in Section 4. This is why maximum torque increment is obtained under conditions when the applied maximum intensity voltage vector and the rotor flux vector are orthogonal (90°). With the increase in speed, the effect of EMF on torque increment intensity becomes very distinct as seen in Figure 7b. The choice of voltage vectors that provide positive torque increments with increasing motor speed becomes very reduced. Only voltage vectors located between 35° and 145° with respect to the rotor flux will provide positive torque increments with diminished intensity in comparison with torque increments at zero motor speed. At the same time, negative torque changes are much higher as the induced EMF supports the decrease of the machine torque within the Δt . Due to this effect, in the ST-DTC methods without regulating PI structures or other EMF compensation techniques, a torque error occurs at high speed. The intensity of this error depends directly on the induced EMF, that is, the motor speed as seen in Figure 8a.

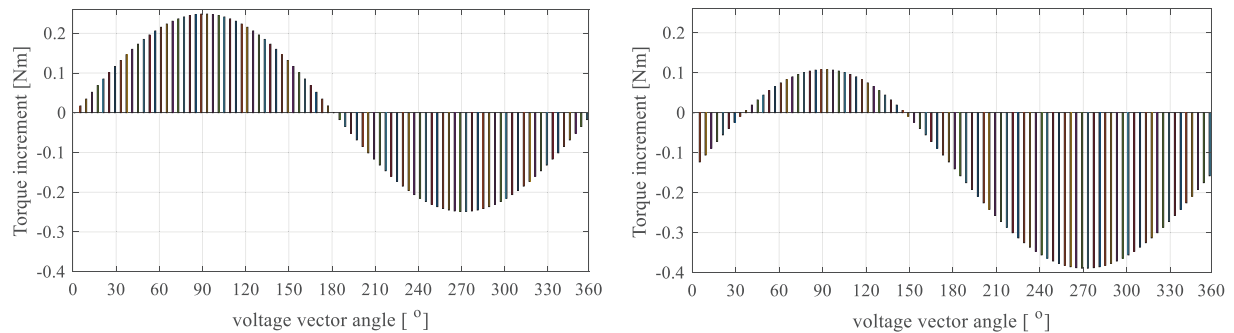


Figure 7. Torque increments depending on voltage vector direction in $\alpha\beta$ reference plane at $\omega=0$ p.u. (a) and $\omega=1$ p.u. (b).

3.2. Feed-forward compensation of speed (EMF) impact

For speed-regulated systems, the torque error is not of great importance, while in the systems where only torque control loop exists, it represents a serious defect. In order to eliminate this effect, the authors in [28–30] propose the definition of a nonsymmetric torque comparator. The disparity of such a comparator allows the use of different intensities of the voltage vector if the torque error is positive or negative. In this way, the EMF effect is compensated by applying the higher intensity voltage, but the adequate compensation of the EMF is possible only for certain speeds. If the boundaries of the asymmetric comparator are not adaptive in terms of motor speed, the steady-state torque error will not be successfully compensated. Also, at low speed, the machine

torque will have values greater than the reference one. The authors in [31] present dynamic hysteresis torque band comparator aiming to deal with the issue. By defining an EMF range subdivision with an appropriate number of levels [13], it is possible to take into account the motor speed in selection of the voltage vector. However, the disadvantage of this method is torque ripple variation with the change in the motor speed.

Since the induced EMF value ($j\omega\Psi_s$) in (4) depends on the motor speed and the stator flux components of a machine in the $\alpha\beta$ coordinate system, it is possible to carry out the accurate EMF compensation very easily [32]. The resulting voltage that compensates the EMF effect is calculated according to (5):

$$\mathbf{u}_{s\text{res.}} = \mathbf{u}_s + \mathbf{u}_{\text{add.}} = \mathbf{u}_s + j\omega\Psi_s = u_{\alpha s} + ju_{\beta s} + j\omega(\psi_{\alpha s} + j\psi_{\beta s}) = \underbrace{u_{\alpha s} - \omega\psi_{\beta s}}_{\text{Re}(\mathbf{u}_{s\text{new}})} + j\underbrace{(u_{\beta s} + \omega\psi_{\alpha s})}_{\text{Im}(\mathbf{u}_{s\text{new}})}. \quad (5)$$

The added EMF value to the selected predefined voltage vector (depending on torque error intensity) forms the resulting voltage vector. With described feed-forward compensation the EMF effect on torque increments is eliminated without implementation of PI control structures, which usually introduce additional calculations, and appropriate parameter tuning that determines the control system performance [2, 33, 34]. More importantly, the resulting torque ripple will not depend on the motor speed, but only on the number of available voltage vectors. Removing the EMF impact on torque increments will ensure proper analysis of torque ripple reduction depending on the number of defined voltage vector intensities at any motor speed. Torque attenuation stemming from the machine parameters (3) is also taken into account in the torque error calculation in this paper. By introducing a parameter k (slightly less than 1) that has been calculated before the DVI-DTC algorithm is executed, the torque error is calculated as follows (6):

$$T_{err.} = T_{ref.} - T_e + T_{e1} = T_{ref.} - T_e + T_e \left(\frac{1}{\tau_s} + \frac{1}{\tau_r} \right) \frac{\Delta t}{\sigma} = T_{ref.} - k \cdot T_e, \quad (6)$$

where $T_{err.}$ is torque error and $T_{ref.}$ is torque reference. The torque response simulation results of DVI-DTC algorithm with 4 voltage intensities with and without EMF compensation obtained in MATLAB/Simulink are shown in Figure 8. The results illustrate the effectiveness of the feed-forward EMF compensation.

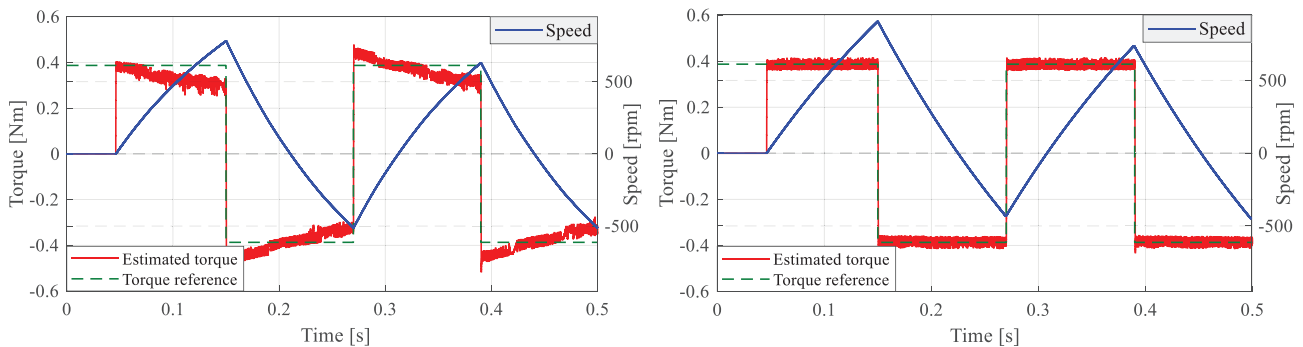


Figure 8. Simulation results of torque response with 4 voltage vector intensities without (a) and with compensated EMF (b).

4. Experimental results

Proposed DVI-DTC algorithms have been tested on the DSP platform MSK2812 together with the conventional DTC in order to compare the obtained results. The MSK2812 platform consists of two-level voltage source inverter module with 6 IGBT switches and 310 V DC bus. The platform is run by TMS320F2812 fixed point processor (150 MHz). The complete experimental setup is shown in Figure 9. The induction machine parameters are given in Table 1.

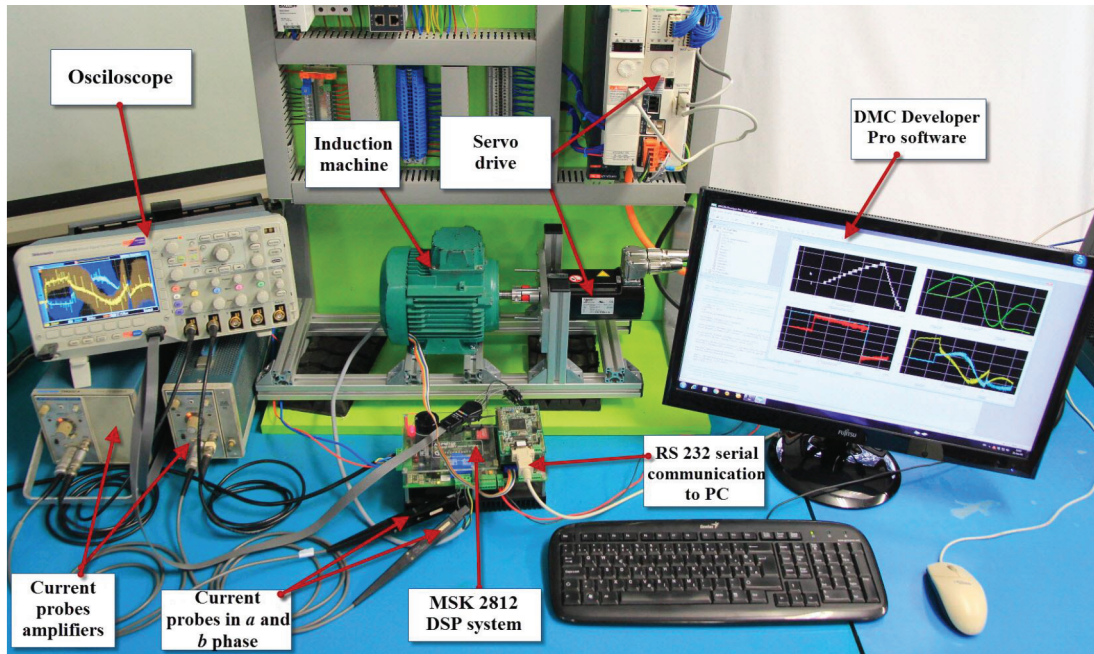


Figure 9. Experimental setup and induction machine parameters.

Table 1. SIEBER LS71 Induction machine parameters.

U_n [V]	400	R_s [Ω]	24.6
I_n [A]	0.95	R_r [Ω]	16.1
P_n [W]	370	L_m [H]	1.46
n_n [rpm]	2860	L_s [H]	1.48
p [pole pairs]	1	L_r [H]	1.48

Gopinath style flux observer which combines voltage and current machine model, presented in [35, 36], is used for the flux estimation. This flux estimation method exhibits excellent results in terms of estimation accuracy where machine parameters mismatch exists, compared to other flux estimation techniques. It also allows flux estimation at wide speed range, including zero while preserving the estimation dynamics.

4.1. Switching frequency of the conventional and DVI-DTC

For the purpose of the comparison of the results, and torque ripple analysis, both conventional DTC and DVI-DTC are set to have the same switching frequency of 20 kHz. However, conventional DTC algorithm

operates at variable switching frequency, but in digital implementation the minimum time between the changes in inverter states is the sampling time of the algorithm. In order to make the results comparable, a modified conventional DTC with fixed switching frequency is used. Instead of using full voltage vector, the algorithm applies the voltage vector with 95% intensity. Although slightly reduced full voltage intensity per each of six basic directions is used, this ensures a change of inverter switching state before next switching period. For zero voltage vectors generation, inverter state 111 is applied for one half of the switching period followed by the 000 state for the remaining part. The described modifications result in two switching states per inverter leg within each switching period of $\Delta t = 50 \mu\text{s}$. All necessary DTC calculations are done within one $\Delta t = 50 \mu\text{s}$ cycle.

The same experimental conditions are ensured for the proposed DVI-DTC by use of SVPWM with defined switching frequency of 20 kHz ($50 \mu\text{s}$). On the other hand, increase of torque ripple in conventional DTC can be attributed to the time discretization of the algorithm, as the discrete-time hysteresis comparators [34] introduce one sample time delay in the selected voltage vector application to the motor terminals. The same one sample time delay exists in DVI-DTC algorithm, but with lower influence on the torque ripple thanks to low intensity voltage vectors.

4.2. Parallel offline torque estimation

Experimentally obtained torque responses are presented along with the results obtained with parallel offline torque estimation using the oscilloscope (OSC) for collecting the data sampled with higher frequency. The parallel torque estimation was performed by multiple sampling of the stator current, providing the flux and torque values between the two sampling instances on the DSP (estimated torque values within $\Delta t = 50 \mu\text{s}$ time frame - Figure 10). The parallel offline torque estimation was done in MATLAB with the identical estimator implemented in the DSP.

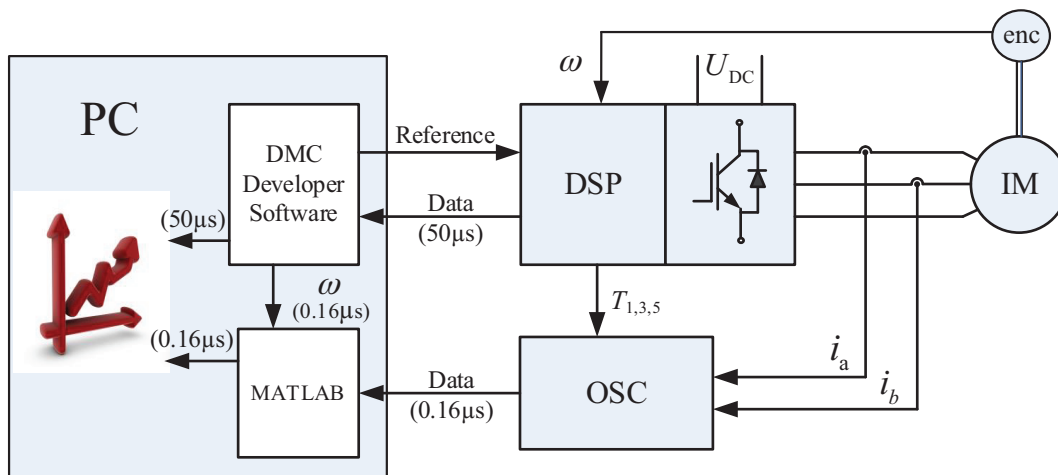


Figure 10. Parallel flux and torque estimation with oversampled current values by oscilloscope - OSC (6.25 MHz).

Figure 11 shows obtained responses of the machine to the cyclic change of torque reference ($\pm 0.3 \text{ p.u}$) for the conventional DTC and DVI-DTC without (Figure 4b) and with EMF compensation (Figure 4c). Also, the zoomed part of the torque response is given along with the results of the parallel torque estimation. Figure 11 clearly confirms that the resulting torque ripple is approximately 4-5 times smaller with only 4 defined voltage vector intensities compared to the conventional DTC. Smaller torque increments are noticeable between the

two DSP sampling instances (Δt) as a result of applying voltage vectors of significantly lower intensities in the DVI-DTC compared to the conventional DTC(Figure 11 - zoomed part).

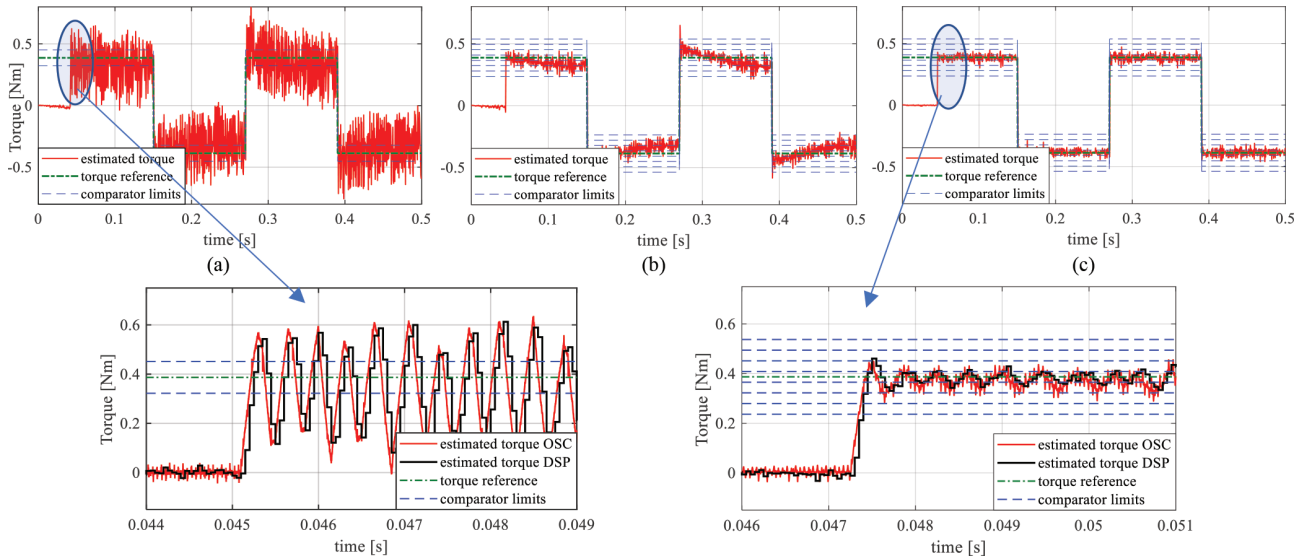


Figure 11. Experimental results of torque response obtained by DSP – 20 kHz and by parallel torque estimation (OSC) – 6.25 MHz for conventional DTC (a) and for DVI-DTC with 4 voltage vector intensities without EMF compensation (b) and with EMF compensation (c).

4.3. Torque ripple reduction analysis

The proposed DVI-DTC algorithm with feed-forward EMF compensation was tested with the defined 3, 4, 5, and 6 discretized voltage intensities in order to determine the reduction degree of the torque ripple. For ripple calculation, the currents and voltages were sampled at $0.16 \mu\text{s}$ (6.25 MHz), and offline torque estimation was performed for the sake of better estimated torque resolution and results comparison. In this way, the practically continuous-time estimated torque signal (312 torque samples within $\Delta t = 50 \mu\text{s}$) was obtained, as shown in Figure 11. For the torque ripple analysis, the time span with more than 600,000 torque values is selected, allowing for more precise assessment of torque ripple thanks to the provided insight into the torque behavior between two DSP sampling instances. The average torque ripple, $T_{av. \text{ ripple}}$, was calculated using the following expressions (7), where m stands for number of torque samples. The obtained results are shown in Figure 12.

$$T_{av. \text{ ripple}} = \sqrt{\frac{1}{m} \sum_{x=1}^m (T_x - T_{av.})^2} \quad ; \quad T_{av. \text{ ripple}} [\%] = \frac{\sqrt{\frac{1}{m} \sum_{x=1}^m (T_x - T_{av.})^2}}{T_r} \cdot 100, \quad (7)$$

where T_x is the sampled torque and T_r is the rated torque.

Figure 12 shows the torque response with the conventional DTC (a) and the proposed DVI-DTC with 4 and 6 voltage intensities (b) to (c) respectively. The torque ripple is calculated as a difference between the estimated torque T_x and average torque value $T_{av.}$ (black line on Figure 12 (left)) during the positive torque reference. The average torque ripple value for the conventional and proposed DVI-DTC methods are presented

both graphically with the blue line in Figure 12 (right) and numerically in Table 2. The results in Table 2 obtained for the DVI-DTC algorithm with disabled and enabled EMF compensation are presented in columns 1 and 2 respectively.

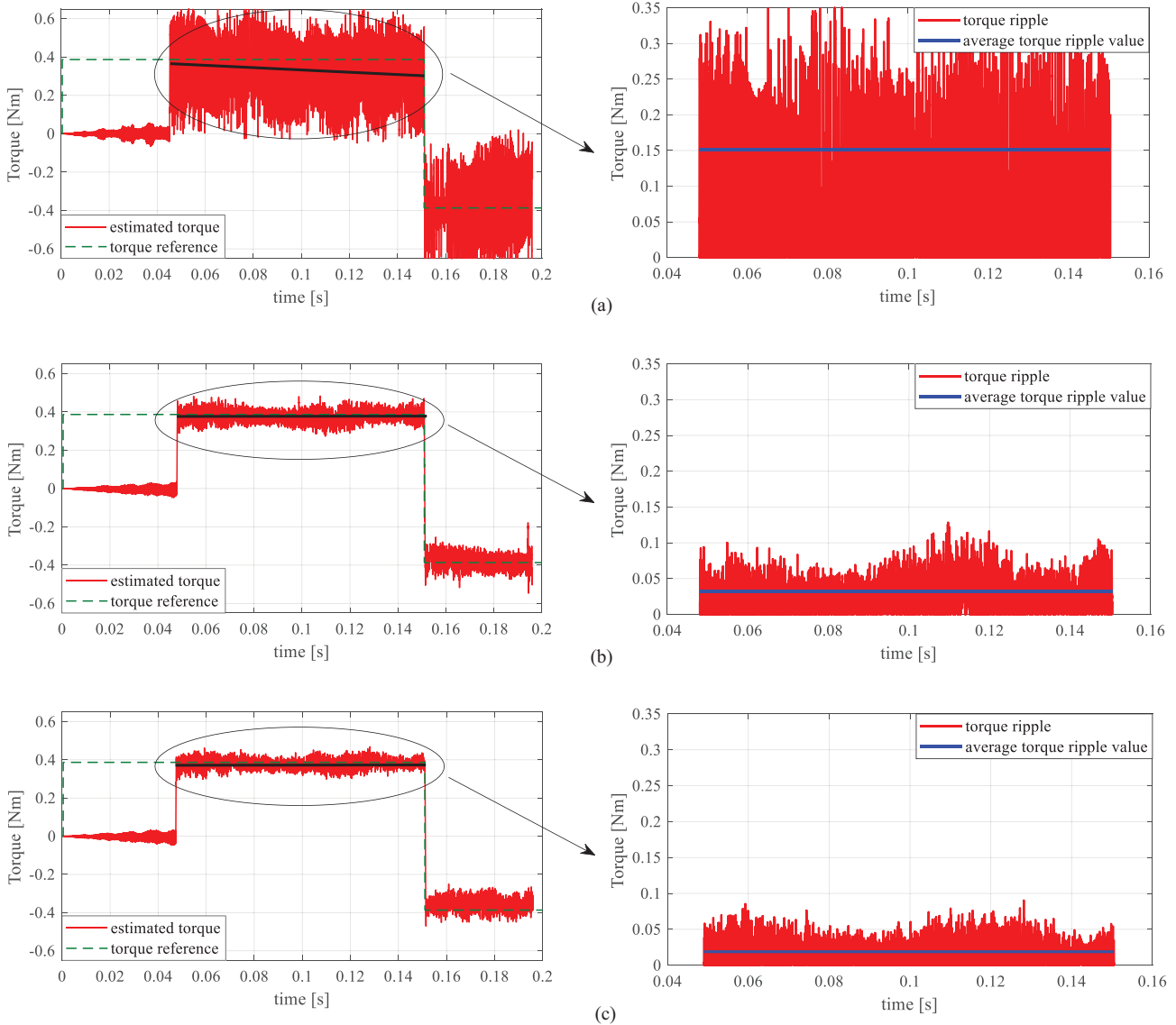


Figure 12. Estimated machine torque in (a) conventional DTC and proposed DVI-DTC algorithm with: 4 (b) and 6 (c) voltage vector intensities (left) and related average torque ripple value (right).

The results confirm a drastic decrease of torque ripple with an increase in the number of available voltage intensities particularly (even more) with compensated EMF. The torque ripple is reduced by a factor of 1.89 in the case of DVI-DTC with 3 voltage vector intensities and compensated EMF compared to conventional DTC. With 4, 5, and 6 voltage vector intensities the torque ripple is reduced by 4.69, 6.95, and 8.06 times, respectively. The results given by Figure 13 shows approximately the exponential reduction of torque ripple as the number of available voltage intensities rises. The presented results lead to a conclusion that the reduction in the torque ripple is approximately to 50%, or to 20% of the value of the torque ripple that is present in the conventional

DTC by defining only 3 or 4 voltage intensities, respectively. The numerical results presented in Table 2 point to the additional conclusion. Torque ripple reduction factor is higher with compensated EMF comparing it to corresponding cases without EMF compensation and the difference between torque ripple reduction factors with and without compensated EMF rises with the number of defined voltage vectors.

Table 2. Numerical torque ripple analysis in conventional DTC and DVI-DTC method

DTC control method	Average torque ripple (Nm)		Torque ripple / rated torque (%)		C-DTC / DVI-DTC torque ripple ratio	
	1	2	1	2	1	2
Conv. DTC	0.1515		11.74		1	
DVI-DTC 3	0.0835	0.0802	6.47	6.21	1.81	1.89
DVI-DTC 4	0.0354	0.0323	2.74	2.5	4.28	4.69
DVI-DTC 5	0.0262	0.0218	2.03	1.69	5.78	6.95
DVI-DTC 6	0.0234	0.0188	1.81	1.46	6.47	8.06
	<i>1 – EMF compensation disabled; 2 – EMF compensation enabled.</i>					

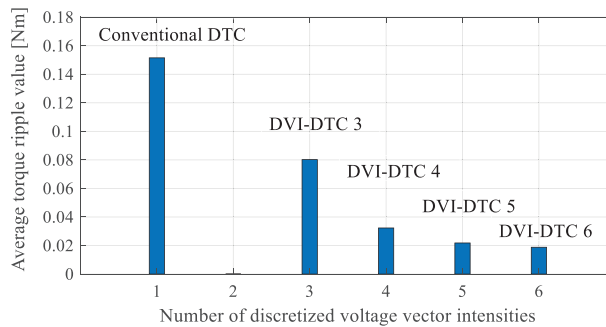


Figure 13. Torque ripple intensity in DVI-DTC depending on the number of available discretized voltage intensities.

5. Conclusions

In this paper, an algorithm with an arbitrary number of discretized voltage intensities has been proposed, which allows for a significant and adjustable torque ripple reduction. The presented DVI-DTC algorithm provides the user with the possibility of changing the number of intensities of the applied voltage vectors in an easy way without altering the basic structure of the algorithm in order to adequately reduce the torque ripple. It has been shown that the increase of the number of defined voltage intensities remarkably reduces the torque ripple. The change in the number of voltage vectors does not introduce new switching tables, since decoupled selection of the direction and the intensity of the voltage vector is inherent. The algorithm is characterized by simplicity without complex calculations, which allows automatic modification of the control structure depending on the desired number of voltage intensities. Performing calculation with the DVI-DTC algorithm lasts only a couple of percent longer (2–5%) compared to the conventional DTC, which represents the simplest form of DTC control. The rapid execution is a consequence of the absence of complex mathematical operations in the proposed DVI-DTC algorithm. EMF impact on torque increments is analyzed and compensated in a simple manner. The EMF compensation provides a condition for more accurate analysis of the machine torque ripple where torque

ripple depends exclusively on the number of discretized voltage vector intensities. The presented results confirm higher torque ripple reduction in cases where EMF compensation is enabled.

Acknowledgment

This study was supported by the Ministry of Education, Science and Technological Development of the Republic of Serbia, and these results are parts of the Grant No. 451-03-68/2020-14/200132 with University of Kragujevac - Faculty of Technical Sciences Čačak.

References

- [1] Zhang Y, Zhu J, Xu W, Guo Y. A simple method to reduce torque ripple in direct torque-controlled permanent-magnet synchronous motor by using vectors with variable amplitude and angle. *IEEE Transaction on Industrial Electronics* 2011; 58 (7): 2848-2859. doi: 10.1109/TIE.2010.2076413
- [2] West NT, Lorenz RD. Implementation and evaluation of a stator and rotor flux linkage-based dead-beat, direct torque control of induction machines at the operational voltage limits. In: 2007 IEEE Industry Applications Annual Meeting; New Orleans, LA, USA; 2007. pp. 690-695. doi: 10.1109/07IAS.2007.109
- [3] Belkacem S, Naciri F, Abdessemed R. Reduction of torque ripple in DTC for induction motor using input-output feedback linearization, *Turkish Journal of Electrical Engineering & Computer Sciences* 2012; 20 (3): 273-285. doi: 10.3906/elk-1007-596
- [4] Kumar RH, Iqbal A, Lenin NC. Review of recent advancements of direct torque control in induction motor drives a decade of progress. *IET Power Electronics* 2018; 11(1): 1-15. doi: 10.1049/iet-pel.2017.0252
- [5] Casadei D, Serra G, Tani A, Zarri L. Assessment of direct torque control for induction motor drives. *Bulletin of the Polish Academy of Sciences: Technical Sciences* 2006; 54 (3): 237-254.
- [6] Adel AH, Refky A, Abo-Zaid S, Elwany M. Torque ripple reduction in direct torque control of induction motor drives by improvement of the switching table. *Journal of Multidisciplinary Engineering Science and Technology* 2014; 1 (5): 238-243.
- [7] Korkmaz F. Performance improvement of induction motor drives with model-based predictive torque control. *Turkish Journal of Electrical Engineering & Computer Sciences* 2020; 28(1): 525-539. doi: 10.3906/elk-1804-124
- [8] Kodumur Meesala RE, Thippiripati VK. An improved direct torque control of three-level dual inverter fed open-ended winding induction motor drive based on modified look-up table. *IEEE Transactions on Power Electronics* 2020; 35 (4): 3906-3917. doi:10.1109/TPEL.2019.2937684.
- [9] Purcell A, Acarnley P. Device switching scheme for direct torque control. *Electronics Letters* 1998; 34 (4): 412-414. doi: 10.1049/el:19980256
- [10] Casadei D, Serra G, Tani A. Improvement of direct torque control performance by using a discrete SVM technique. In: PESC 98 Record. 29th Annual IEEE Power Electronics Specialists Conference (Cat. No.98CH36196); Fukuoka, Japan; 1998. pp. 997-1003. doi: 10.1109/PESC.1998.703125
- [11] Casadei D, Serra G, Tani A. Analytical investigation of torque and flux ripple in DTC schemes for induction motors. In: Proceedings of the IECON'97 23rd International Conference on Industrial Electronics, Control, and Instrumentation (Cat. No.97CH36066); New Orleans, LA, USA; 1997. pp. 552-556. doi: 10.1109/IECON.1997.671793
- [12] Casadei D, Serra G, Tani A. Implementation of a direct control algorithm for induction motors based on discrete space vector modulation. *IEEE Transactions on Power Electronics* 2000; 15 (4): 769-777. doi: 10.1109/63.849048
- [13] Betin F, Capolino GA, Casadei D, Kawkabani B, Bojoi RI et. al. Trends in electrical machines control: Samples for classical, sensorless, and fault-tolerant techniques. *IEEE Industrial Electronics Magazine* 2014; 8 (2): 43-55. doi: 10.1109/MIE.2014.2313752

- [14] Rodríguez J, Lai JS, Peng FZ. Multilevel inverters: A survey of topologies, controls, and applications. *IEEE Transactions on Industrial Electronics* 2002; 48 (4): 724-738. doi: 10.1109/TIE.2002.801052
- [15] Naganathan P, Srinivas S, Ittamveetil H. Five-level torque controller-based DTC method for a cascaded three-level inverter fed induction motor drive. *IET Power Electronics* 2017; 10 (10): 1223-1230. doi: 10.1049/iet-pel.2016.0614
- [16] Khoucha F, Lagoun MS, Kheloui A, Benbouzid MEH. A comparison of symmetrical and asymmetrical three-phase H-bridge multilevel inverter for DTC induction motor drives. *IEEE Transaction on Energy Conversion* 2011; 26 (1): 64-72. doi: 10.1109/TEC.2010.2077296
- [17] Mohan D, Zhang X, Beng Foo GH. Generalized DTC strategy for multilevel inverter fed IPMSMs with constant inverter switching frequency and reduced torque ripples. *IEEE Transaction on Energy Conversion* 2017; 32 (3): 1031-1041. doi: 10.1109/TEC.2017.2681653
- [18] Zheng L, Fletcher JE, Williams BW, He X. A novel direct torque control scheme for a sensorless five-phase induction motor drive. *IEEE Transaction on Industrial Electronics* 2011; 58 (2): pp. 503-513. doi:10.1109/TIE.2010.2047830.
- [19] Pandit JK, Aware MV, Nemade RV, Levi E. Direct torque control scheme for a six-phase induction motor with reduced torque ripple. *IEEE Transactions on Power Electronics* 2017; 32 (9): 7118-712. doi: 10.1109/TPEL.2016.2624149
- [20] Sharma S, Aware M, Bhowate A, Levi E. Performance improvement in six-phase symmetrical induction motor by using synthetic voltage vector based direct torque control. *IET Electric Power Applications* 2019; 13 (11): 1638-1646. doi: 10.1049/iet-epa.2018.5983
- [21] Sutikno T, Idris NRN, Jidin A, Cirstea MN. An improved FPGA implementation of direct torque control for induction machines. *IEEE Transactions on Industrial Informatics* 2013; 9 (3): 1280-1290. doi: 10.1109/TII.2012.2222420
- [22] Bae B, Sul S. A compensation method for time delay of full-digital synchronous frame current regulator of pwm ac drives. *IEEE Transactions on Industry Applications* 2003; 39 (3): 802-810. doi: 10.1109/TIA.2003.810660
- [23] Aktaş M, Okumuş Hİ. Stator resistance estimation using ANN in DTC IM drives. *Turkish Journal of Electrical Engineering & Computer Sciences* 2010; 18 (2): 197-210. doi: 10.3906/elk-0812-6
- [24] Suresh S, Rajeevan PP. Virtual space vector-based direct torque control schemes for Induction Motor Drives. *IEEE Transactions on Industry Applications* 2020; 56(3): 2719-2728. doi: 10.1109/TIA.2020.2978447
- [25] Arumugam S, Thathan M. Novel switching table for direct torque controlled permanent magnet synchronous motors to reduce torque ripple. *Journal of Power Electronics* 2013; 13 (6): 939-954. doi: 10.6113/JPE.2013.13.6.939
- [26] Vas P. Direct torque control (DTC) of induction machines. In: Vas P (editor). *Sensorless Vector and Direct Torque Control*. Oxford, United Kingdom: Oxford University Press, 1998, pp. 505-574.
- [27] Ren Y, Zhu ZQ, Liu JM. Direct torque control of permanent-magnet synchronous machine drives with a simple duty ratio regulator. *IEEE Transaction on Industrial Electronics* 2014; 61 (10): 5249-5258. doi: 10.1109/TIE.2014.2300070
- [28] Leong JH, Zhu ZQ, Liu JM. Minimization of steady-state torque tracking error in direct-torque controlled PM brushless AC drives. In: 2013 Eighth International Conference and Exhibition on Ecological Vehicles and Renewable Energies (EVER); Monte Carlo, Monaco; 2013. pp. 1-4. doi: 10.1109/EVER.2013.6521612
- [29] Rosic M, Jeftenic B, Bebic M. Reduction of torque ripple in DTC induction motor drive with discrete voltage vectors. *Serbian Journal of Electrical Engineering* 2014; 11 (1): 159-173. doi: 10.2298/SJEE131204014R
- [30] Alsofyani IM, Kim KY, Lee SS, Lee K. A modified flux regulation method to minimize switching frequency and improve DTC-hysteresis-based induction machines in low-speed regions. *IEEE Journal of Emerging and Selected Topics in Power Electronics* 2019; 7(4): 2346-2355. doi:10.1109/JESTPE.2019.2897064.
- [31] Alsofyani IM, Idris NRN, Lee K. Dynamic Hysteresis torque band for improving the performance of lookup-table-based DTC of Induction Machines. *IEEE Transactions on Power Electronics* 2018; 33(9): 7959-7970. doi: 10.1109/TPEL.2017.2773129

- [32] Rosic M, Bjekic M, Bebic M, Jeftenic B. Electromotive force compensation in direct torque control with discretized voltage intensities. In: 2016 4th International Symposium on Environmental Friendly Energies and Applications (EFEA); Serbia, Belgrade; 2016. pp. 1-6. doi:10.1109/EFEA.2016.7748810.
- [33] T. Yuan et al. Duty ratio modulation strategy to minimize torque and flux linkage ripples in IPMSM DTC systems. IEEE Access 2017; 1: 14323-14332. doi: 10.1109/ACCESS.2017.2732683
- [34] Buja G, Kazmierowski M. Direct torque control of PWM inverter-fed AC motors - a survey. IEEE Transaction on Industrial Electronics 2004; 51 (4): 744-757. doi: 10.1109/TIE.2004.831717
- [35] Jansen PL, Lorenz RD, A physically insightful approach to the design and accuracy assessment of flux observers for field oriented induction machine drives, IEEE Transaction on Industry Applications 1994; 30 (1): 101-110. doi: 10.1109/28.273627
- [36] Heinbokel BE, Lorenz RD. Robustness evaluation of deadbeat, direct torque and flux control for induction machine drives. In: 2009 13th European Conference on Power Electronics and Applications; Barcelona, Spain; 2009. pp. 1-10.